

SHEFFIELD HALLAM UNIVERSITY

Faculty of Arts, Computing, Engineering and
Sciences

**Application of Attractor
Reconstruction to Epileptic Seizure
Onset Detection**

*A thesis submitted in partial fulfilment of the requirements
for the degree of Master of Science*

in

Telecommunication and Electronic Engineering

Submitted by:

Shehan

Dharmadasa

Supervisor:

Dr. Chathuranga

Weeraddana

October 16, 2017

Preface

This report describes project work carried out in the Faculty of Arts, Computing, Engineering and Sciences at Sheffield Hallam University between September 2012 to December 2015.

The submission of the report is in accordance with requirements for the awards of degree of Master of Science in Telecommunication and Electronic Engineering under the auspices of the University.

Acknowledgements

Human beings are born with talents and abilities. I thank my God for the ability, strength to go on when it seemed so difficult, and the relentless will to achieve, and also for putting me across the path of my supervisor.

We always stand on the shoulders of those who have gone before us, and in this instance I wish to express my profound gratitude to my supervisor Dr. Chathuranga Weeraddna for his expertise, understanding, generous guidance, and support.

I also wish to thank Dr. Dilshani Dissanayake, of the Department of Physiology, Faculty of Medicine, University of Colombo for the fruitful discussion on epileptic seizures.

Abstract

Epilepsy is a disorder of the central nervous system that causes individuals suffering from it to undergo recurrent seizures. It affects over 50 million people worldwide.

A seizure is an abrupt anomaly in electrical activity, that disrupts the normal working of the brain. Symptoms of epileptic seizures can range from simple disorientation and lapse in attention, to sensory hallucinations and to full-body convulsion. One third of patients with epilepsy continue to suffer with seizures despite treatment. Such patients have their mobility and independence severely limited and thereby undergo economic hardship and social isolation. More seriously such patients have a much higher risk of experiencing burns, lacerations, fractures and even death.

This thesis presents a method of detecting epileptic seizures as they happen, with the objective that when a such a seizure is detected a caregiver or paramedic may be alerted to prevent any injury to the patient as a result of the seizure. At the heart of the presented method is an automated method for seizure detection based on the patients electroencephalogram (EEG). The presented method works by attempting to recreate a non linear dynamical system which could have generated the the EEG of the patient at a given moment of time. The method was tested on 100 hours of pre recorded scalp EEG data from 10 paediatric epilepsy patients and reported a sensitivity of 91% with a mean detection time of 3.6 seconds

Contents

Preface	i
Acknowledgements	ii
Abstract	iii
1 Introduction	1
1.1 Epilepsy	1
1.2 Motivation	3
1.3 Challenges	4
1.4 Objectives	4
2 Literature Review	5
2.1 Electroencephalogram Analysis Methods for Epileptic Seizure Detection	5
2.2 Time Domain Methods	6
2.3 Frequency Domain Methods	6
2.4 Time-Frequency Domain Methods	8
2.5 Information Theory Based Methods	9
2.6 Non-Linear Methods	10
3 Theoretical Background	12
3.1 The Electroencephalogram	12

3.2	Epilepsy And The EEG	13
3.3	Non Linear Brain Dynamics	18
3.4	Dynamical systems	20
3.5	Phase Space	21
3.6	Attractors	21
3.7	Characterisation of attractors - Lyapunov Exponents	23
3.8	Embedding - Attractor Reconstruction	25
3.9	Optimum Embedding Parameter Estimation	26
3.10	Non Linear Analysis of the Epileptic Seizures	28
4	Methodology	30
4.1	Epoching of EEG Data	30
4.2	Preprocessing of EEG Data	30
4.3	Smoothed EEG Subtraction	31
4.4	EEG Channel Fusion	32
4.4.1	The FFT Approximation Method of Lehmann and Michel	32
4.4.2	Global Field Power	33
4.4.3	The Stockwell Transform	34
4.5	Identification Of Changes in Optimum Embedding Parameters . .	36
5	Materials and Testing	37
5.1	The EEG Data Set	37
5.2	Preliminary Testing Of The Proposed Method	38
5.3	Detecting Changes in Optimum Embedding Parameters - Preliminary Tests	38
5.3.1	Results From Patient No. 3 - Seizure record	38
5.3.2	Results From Patient No. 3 - Non Seizure record	40

5.3.3	Results From Patient No. 5 - Seizure record	41
5.3.4	Results From Patient No. 5 - Non Seizure record	44
5.3.5	Results From Patient No. 9 - Seizure record	46
5.3.6	Results From Patient No. 9 - Non Seizure record	48
5.4	Analysis Of Preliminary Results	49
5.5	Further Processing For Automatic Blind Detection of Seizures . .	50
5.5.1	Calculation Of Detection Threshold	50
5.5.2	Detection Delay	51
5.6	Final Testing of the Proposed Method	52
5.6.1	Performance Metrics	52
5.6.2	Detector Performance	53
	Detection Delay	53
	Sensitivity	54
6	Conclusions And Future Work	55
6.1	Conclusions	55
6.2	Future Work	56

List of Figures

3.1	The international 10-20 system	13
3.2	Progression of clinical symptoms of an epileptic seizure	15
3.3	EEG pattern of generalized seizure	16
3.4	EEG pattern of generalized seizure	17
3.5	EEG pattern of absence seizure	18
3.6	Different types of attractors	23
4.1	Sine - Cosine plot	33
4.2	Orthogonal projections onto the single dipole FFT approximation line	33
5.1	Optimum embedding dimension, patient 3, record no. 1	39
5.2	Zoom in to seizure occurring in figure 5.1	39
5.3	EEG at start of seizure, patient 3, record no. 1	40
5.4	Optimum embedding dimension, patient 3, record no. 14	40
5.5	Optimum embedding dimension, patient 5, record no. 17	42
5.6	Zoom in to seizure occurring in figure 5.5	42
5.7	EEG at start of seizure, patient 5, record no. 17	43
5.8	EEG, 2657s - 2665s, patient 5, record no. 17	43
5.9	EEG, 3187s - 3195s, patient 5, record no. 17	44
5.10	EEG, 3507s - 3515s, patient 5, record no. 17	44
5.11	Optimum embedding dimension, patient 5, record no. 4	45

5.12	Zoom in of unexpected seizure in figure 5.11	45
5.13	EEG, 2815s - 2823s, patient 5, record no. 17	46
5.14	Optimum embedding dimension, patient 9, record no. 8	47
5.15	Zoom in to seizure occurring in figure 5.14	47
5.16	EEG at start of seizure, patient 9, record no. 2	48
5.17	Optimum embedding dimension, patient 9, record no. 2	49
5.18	Application of threshold detection to record no. 14, patient 5 . . .	51
5.19	Distribution of seizure and non seizure records across the 10 patients	52
5.20	Seizure detection delays for the 10 patients in the test	54
5.21	Detector sensitivity for the 10 patients	54

Chapter 1

Introduction

1.1 Epilepsy

Epilepsy is a disorder of the central nervous system that causes individuals suffering from it to undergo recurrent seizures. A seizure is an abrupt anomaly in electrical activity that disrupts the normal working of the brain. Symptoms of epileptic seizures can range from simple disorientation and lapse in attention, to sensory hallucinations and to full-body convulsion. The poet Stuart Ross McCallum describes the onset of a seizure:

It's here again, the sinister sensation of an aura that I know only too well.

Searching for a safe place to lay down as I descend into my private hell.

I shout out loud, "It's happening again," it's beyond my control.

Dropping down heavily, my head hits the floor.

Feeling horrid my mind and body is no longer in my control.

Twitching, shaking, and staring into space – I blackout.

Epilepsy is not a singular disease but belongs to a family of syndromes that share the common feature of recurring seizures. Physiological causes of epilepsy could be the inheritance of a mutation in the molecular mechanism that

regulates neuron connectivity, brain trauma due to injury, stroke, and infections of the cerebellum or malignancies of the brain [Brown1992].

Epilepsy occurs with an incidence of 6.88/100,000 person-years [Christensen2007], and the age adjusted incidence of epilepsy is estimated to be 44/100,000 person-years [Hauser1993], thereby making epilepsy one of the most common neurological disorders. Although new anti-epileptic drugs have been developed over the past few decades, one third of patients with epilepsy continue to suffer with seizures despite treatment [Kwan2000]. Such patients have their mobility and independence severely limited and thereby undergo economic hardship and social isolation. More seriously such patients have a much higher risk of experiencing burns, lacerations, fractures and even death [Friedman2010][Ficker2000]. In patients whose epilepsy is controlled by medication, the anxiety caused by the unpredictable nature of the condition results in a reported lower quality of life [Camfield2010].

They don't know

Know what it feels like

Every day

Pain, suffering, weakness.

You look great on the outside

But you feel terrible on the inside

All the pain!

It hurts but you wouldn't know!

You can't feel it

The pain suffering and weakness!

It hurts so bad!

All I want to do is sleep

Excerpt from: My Epilepsy Life - Poem by Felicia Nicole Haggard, Chattanooga, Tn, USA.

The negative effects of epilepsy apply not only the individual sufferers but also to their families, friends and co-workers. The families of epilepsy patients undergo chronic anxiety, and need to rearrange their lives so that the safety of their loved one is ensured. The estimated annual direct medical cost of epilepsy in the United States, not considering indirect costs from losses in productivity and quality of life, is \$ 9.6 billion [England2012]. Therefore novel therapeutic methods that can better control seizures as well as technology which help both the affected individual as well as their care givers to cope with the arising consequences of the disease are desperately needed.

1.2 Motivation

The ability of an automated system to detect the onset of a seizure may ease the burden that is carried by sufferers of medically intractable epilepsy, by being able to warn them of the impending seizure just prior to the onset of debilitating symptoms, or could alert those nearby of what is to come so that the consequences of the seizure may be mitigated. Therapeutic systems may be able to reduce symptoms or even abort a seizure through automated and targeted administration of treatment with accurate detection of the onset of a seizure.

1.3 Challenges

Detection of the onset of a seizure is usually accomplished through the analysis of the electroencephalogram or EEG, which is a recording of the electrical activity that is generated by the billions of neurons of the brain. The different channels of the EEG reflect the electrical activity of different parts of the brain at a given moment in time. The EEG that is recorded by placing electrodes on an individual's scalp is called the scalp EEG, while that which is recorded by invasively placing electrodes directly on the brain is called the intracranial EEG or iEEG. The variability of the EEG across different patients as well as the variation of the EEG among different recordings from the same patient for patterns generated for both seizure and non seizure events make the detection of epileptic seizures from the EEG most challenging.

At the onset of an epileptic seizure, a set of EEG channels will develop rhythmic activity that is caused by the synchronous firing of neurons beneath the electrodes of the channels involved. The location of this rhythmic activity as well as its spectral content shows both inter patient as well as intra patient variability. Also the EEG pattern of a seizure of one patient may resemble non seizure activity from another patient.

1.4 Objectives

The objective of this work is to develop an epileptic seizure detection system based on attractor reconstruction by applying the theories of non-linear dynamics to the EEG. A further objective is to make this detection method independent of inter patient variability to the most possible degree.

Chapter 2

Literature Review

This chapter reviews recent publications involved in the automated detection of epileptic seizures from the EEG.

2.1 Electroencephalogram Analysis Methods for Epileptic Seizure Detection

In the early days of EEG analysis for the purpose of automated epileptic seizure detection (i.e. the 1970s), detection methods relied on interpretation of the EEG using descriptive and heuristic methods. In time however various new methods were developed and used to analyse the subtle changes in the EEG signal which could indicate an epileptic seizure. These methods can be broadly grouped into the following four categories:

1. Time domain methods
2. Frequency domain methods
3. Time-Frequency domain methods
4. Information Theory based methods
5. Non-Linear methods

2.2 Time Domain Methods

In order to detect seizures from the EEG in the time domain, the discrete time sequences of EEG epochs must be analysed. This can usually be accomplished by calculating the histograms of the epochs. Runarsson and Sigurdsson have presented a simple time domain based method through which a seizure is detected by first breaking the signal into half waves and then tracing the maxima and minima of the if the current EEG epoch. The bivariate histogram of the amplitude difference between of consecutive maxima and minima, and the time difference between consecutive maxima and minima is then calculated [Runarsson2005]. A support vector machine is used to classify seizure and non-seizure conditions, and the authors reported a sensitivity of 90%.

Alutnay et al. [Altunay2010] used a linear predictive filter (LPC) to model the EEG signal at a given EEG epoch. The error energy between the actual EEG signal at the given epoch and the predicted signal is then compared to a threshold to detect a seizure. Since the LPC assumes that the signal is stationary it is unable to track sudden spikes, and therefore shows an increase in error energy during ictal periods. A sensitivity of 92% was obtained.

2.3 Frequency Domain Methods

Rana et al. [Rana2012] has presented a frequency domain based epileptic seizure detection method based on the phase slope index (PSI) of the multi-channel iEEG. The PSI is a measure of the weighted sum of the slopes of the phase between two iEEG channels, and is used as measure of the causal influence of one iEEG channel on the other. The authors hypothesise that the

level of causal influence between iEEG channels increases during ictal conditions. The PSI value is then compared against a threshold to test its significance. A global value of interaction between EEG channels is then calculated by summing together the significant PSI values in a given EEG epoch. The global interaction measure is then compared against a threshold to test if a seizure has occurred in the current EEG epoch. Out of the five patients included in the study, the authors were able to detect seizures in four patients with a sensitivity of 100%, while a sensitivity of 93% was reported for the fifth patient. However, the detection latencies for the system averaged slightly less than 20 seconds.

A patient specific seizure detection system by Khamis et al. [Khamis2013] used frequency-moment signatures. Differential EEG signals from electrode pairs T6-P4 for the left hemisphere and T5-P3 for the right hemisphere were first band pass filtered between 0.5 to 50 Hz. A triangular window was used to taper the data to remove unnecessary spectral leakage, and the power spectral densities of the two signals were calculated. Moments of the spectral densities were then used to create seizure and non seizure signatures. The logarithm of the probability that a specific signature belonged to set of non seizure signatures was used as the test metric. A seizure detection sensitivity of 91% and a false alarm rate of 0.02 false positives per hour were reported.

Blanke et al. [Blanke2000] detected seizure onset by first determining the dominant frequencies in the EEG which are related to the seizure, and then observing the EEG until these dominant frequencies arrive. 32 seconds of EEG recording before seizure onset and 14 seconds after seizure onset were used to

create 23 2 second long epochs. The data from each EEG epoch was then transformed into the frequency domain with a resolution of 0.5 Hz using the FFT approximation method of Lehmann and Michel [**Lehmann1990**], to take into account the phase angles between the EEG electrodes, which gives a conclusion about the electric field distribution at each frequency under consideration. This method will be further discussed in Chapter 4. The global field power (GFP) [**Lehmann1980**], which is the the standard deviation of the potentials at all electrodes (obtained from the FFT approximation process) is calculated for each frequency of the FFT. The dominant peaks of the GFP which are consistent across three seizures were determined for each of the EEG epochs, to show how the strength of the electric field at a particular frequency evolves. By following the the evolution of the dominant frequencies back in time, the point where the power in these frequencies begins to rise can be found. this point is considered to be the point of seizure onset.

For the 10 patients analysed, the dominant frequencies were found to be between 3 Hz - 8.5 Hz, The initial rise in dominant frequencies were found to be upto 7 seconds before seizure onset, while the GFP peaked with a maximum latency of 7 seconds.

2.4 Time-Frequency Domain Methods

The method presented by Shoeb [**Shoeb2009**] involved dividing the EEG spectrum of 0 to 30 Hz, from each EEG channel into 8 equal sub bands. The spectral energy in each sub band was then calculated, and the energy measures from each channel were concatenated to form a ‘spatio-spectral’ feature vector. Three consecutive spatio-spectral vectors were then concatenated to form a ‘spatio-spectral-temporal’ feature vector. This is then used to train a support

vector machine in order to classify seizure and non seizure feature vectors. The system was tested on 844 hours of EEG data recorded from 23 patients, and detected 96% of 163 seizures. A false alarm rate of up to 20 false alarms per 24 hours were reported for some patients.

Yan et al. [Yan2015] used the Stockwell transform to get a time-frequency representation of certain iEEG channels involved in a seizure. 10 time-frequency feature vectors are extracted from a 4 second long epoch of EEG data. The feature vector is used to train a gradient boost algorithm based classifier. Post process Kalman filtering is applied to smooth the classifier output, which is then compared to a threshold to detect the occurrence of a seizure. The system was tested on iEEG data from 21 patients and provided an average sensitivity of 94.2% with a mean false detection rate of 0.66 false detections per hour.

2.5 Information Theory Based Methods

Stamoulis et al. [Stamoulis2012] used information theory measures to show that changes in output of the brains neural network at high frequencies precede the onset of focal seizures. EEG data from 7 patients were used from which a total of 39 preictal and 39 ictal epochs which on average were 2 minutes long were extracted. Similarly 42 non-ictal baseline epochs were also used in this analysis. The Authors were able to show that the relative entropies of preictal and ictal epochs were statistically distinct at frequencies greater than 100 Hz. On patients with certain types of seizures there was a decrease in the directionality of information flow specifically at high frequencies. Similarly a drop in preictal interaction information when compared to ictal and non ictal

epochs were shown in certain patients.

Acharya et al. [Acharya2015] used 13 different entropy measures to investigate the detection of seizures. Normal, interictal and ictal datasets from the University of Bonn EEG database were used, and an Analysis Of Variance (ANOVA) statistical test was used to evaluate the discrimination performance of the entropy measures. The test determines an F-value and a p-value for the three groups of data. The authors were able to show that Renyi's entropy, sample entropy, spectral entropy and permutation entropy had the highest F-values, characterising performance and thus showing significant discrimination among the three datasets.

2.6 Non-Linear Methods

Single neurons are highly non-linear elements [Fell2000] and on a group level further non linearity is introduced into the system by the presence of feedback loops in the processing layers of the brain. Thus techniques provided by non-linear dynamics provide additional information that cannot be measured through linear methods [Stam2005]. A further discussion regarding the EEG and non-linear dynamics will be provided in Chapter 3.

Arabi and He [Arabi2012] embedded the EEG data in phase space using Takens' embedding theorem [Takens1981] using parameters determined by the algorithms of Moon et al [Moon1995] and Cao [Cao1997]. The authors then estimated the correlation integral [Sprott2001], which represents a dimensionality measure of a set of random points in state space. The correlation entropy, which is similar to the mutual information between two data

segments, where a large value shows that there are similar characteristics between the two data sets. The Lempel-Ziv Complexity, which is a measure of the randomness of the data sequences. And finally the Largest Lyapunov exponent, which is a measure of the chaotic behaviour of the sequence. If any of these measures exceed a certain significance threshold, a flag is set.

The non-linear independence between EEG channels is also measured; this is a measure of the level of synchronization between the EEG channels that are considered. Again if the non-linear independence between a pair of channels is greater than a threshold another flag is set. If both flags are set then a seizure alert is issued.

The system was tested of 58 hours of iEEG recordings from two patients, containing 10 seizures with a 50 minute preictal period. Sensitivities of 90% and 96.5% were obtained for the two patients. the false detection rates were 0.06 and 0.055 false detections per hour.

Van Esbroeck et al. [**VanEsbroeck2016**] have introduced the use of the Non-Linear Energy Operator (NLEO) to segment the EEG data into variable sized epochs. The NLEO detects large changes in energy, and the data is segmented at these points where the change in energy occurs. EEG epochs that contain significant information are thus created, thus avoiding pertinent information being distributed among several EEG epochs. The authors then followed the same methods as Shoeb which have been described previously. The authors were able to show a overall improvement of 27% in the false prediction rate when compared to the method of Shoeb.

Chapter 3

Theoretical Background

3.1 The Electroencephalogram

The brain operates via the transmission of electrical discharges between neurons. A non invasive way of monitoring these discharges is by measuring the electrical at certain points on the scalp to give a sum of the electrical activity of the millions of neurons that lie below.

Following the pioneering work of Richard Canton who studied the electrical activity in brains of animals in the 19th century, Hans Berger in 1924 recorded the electrical activity of a human brain for the first time. Berger called his recording of the electrical activity an *electroencephalogram*, which he coined from the two Greek words *enkephalos* meaning brain and *gramma* meaning writing. He noted that these brain waves he had recorded were not completely random, but showed certain regularities and periods.

The scalp recordings of the neuronal activity of the brain, now known as the EEG, measure the potential changes that occur over time between a signal electrode and a reference electrode. These electrical potentials are generated by the activity of

tens of millions of neurons in the area of the brain underneath the electrode. To standardise the spacial mapping of the electrical activity of the different regions of the brain, the International Federation of Societies for Electroencephalography and Clinical Neurophysiology has adopted the 10-20 scalp electrode placement system as shown in Figure 3.1.

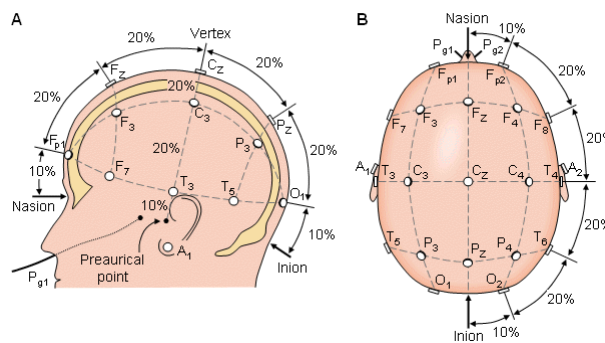


FIGURE 3.1: The international 10-20 system seen from (A) left and (B) above the head. Image from <http://www.bem.fi/book/13/13.htm> - redrawn from **Sharbrough1991**

3.2 Epilepsy And The EEG

Neurons, the cells in the brain, generate, propagate and process electrical signals. Functional networks are formed by interconnections between neurons, and the brain may be viewed as collection of neural networks that interact with each other. Certain neurons exhibit excitatory behaviour, while others show inhibitory activity to inputs to the neural network. Epileptic seizures are caused by temporary hyperactivity and hyper-synchronization of groups of neurons in one or more of the neural networks that make up the brain. These hyperactive and hyper-synchronous states occur due to a temporary imbalance between the excitatory and inhibitory activity of a neural network, favouring excitatory

activity. This imbalance may be caused by interconnectional and intraconnectional defects of the neural networks or by damage to or defects within one or more neurons themselves. These defects may be caused by genetic disorders or by physical trauma to the brain.

Epileptic seizures are usually classified according to the area of the brain from which they originate. For example seizures that originate from a localized area of the brain are known as *focal seizures*. If a focal seizure arises from the area of the brain responsible for emotions and short term memory it may result in hallucinations of taste and smell, feelings of euphoria or fear and paranoia.

Seizures that initiate abnormal electrical activity across the entire brain are known as *generalized seizures*. The effects of such seizures often results in loss of consciousness.

Secondarily generalized seizures are those that begin as a focal seizure and then spread to other areas of the brain and then finally to the whole brain. For example as the seizure spreads to the motor cortex of one side of the brain, it will induce jerks and twitches in the limbs on the opposite sides of the body. As it then spreads to the entire brain whole body convulsion result.

Absence seizures are seizures where there is a loss of cognition and or consciousness with no other physical symptoms.

The progressive clinical symptoms of an epileptic seizure usually show corresponding patterns on the EEG, as shown by Noachtar and Rémi in 2009

[Noachtar2009] in Figure 3.2. Interictal epileptiform discharges are certain EEG patterns that do not normally occur in healthy individuals and tend to precede seizures. There exist however, seizures that do not show any clinical symptoms but only appear on the EEG. These are known as *sub clinical seizures* [Bromfield2006].

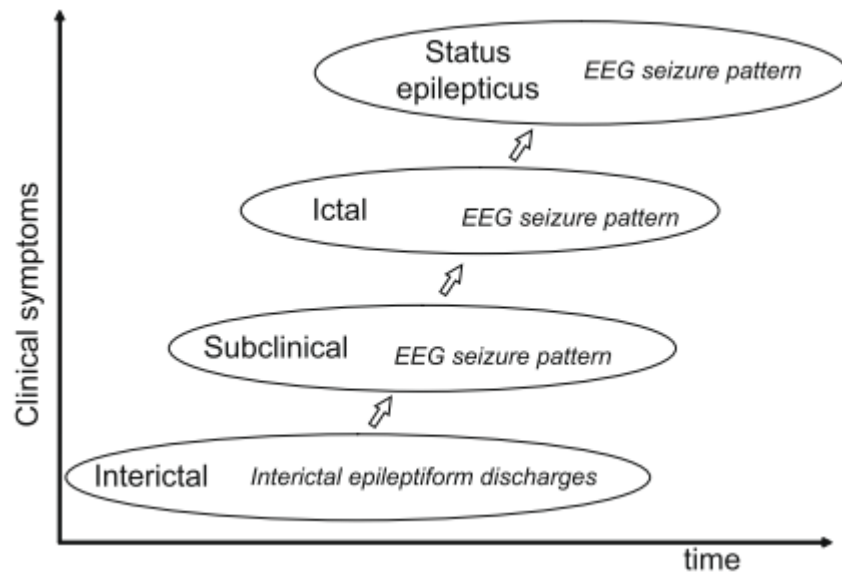


FIGURE 3.2: Progression of clinical symptoms of an epileptic seizure with corresponding EEG pattern [Noachtar2009]

The following figures show typical seizure patterns of three paediatric epilepsy patients.

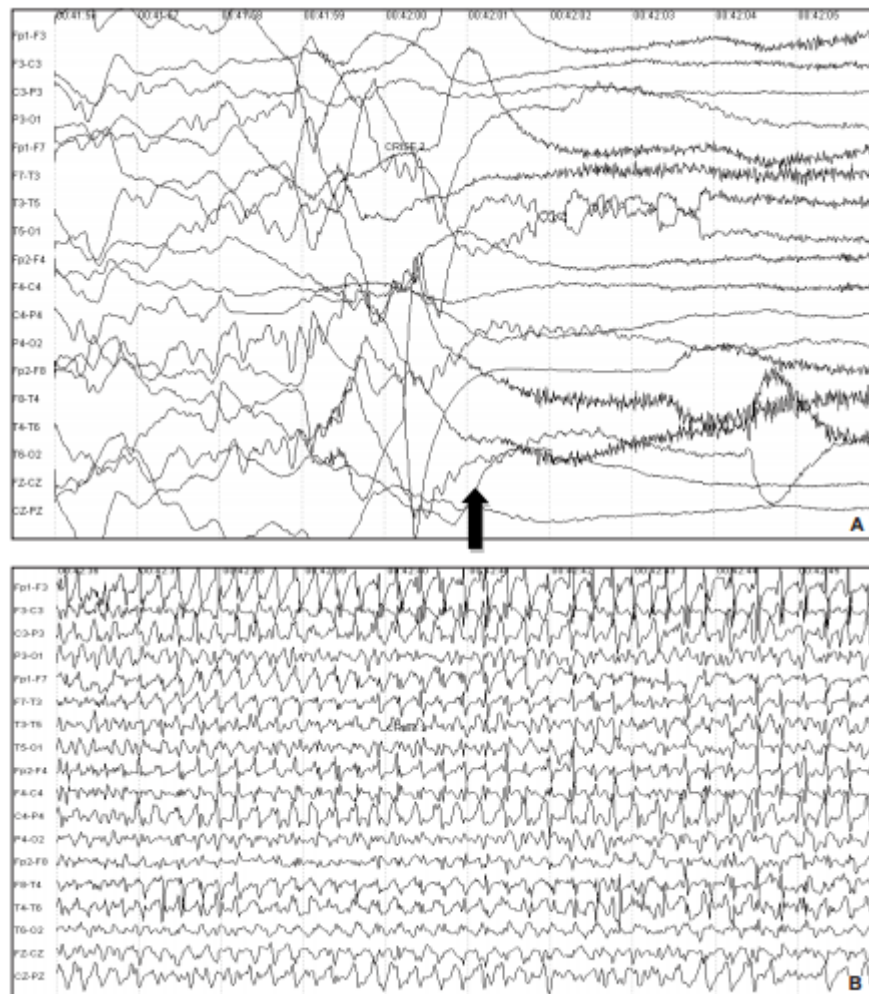


FIGURE 3.3: EEG of a generalized seizure from paediatric patient
A. Beginning of seizure marked with arrow (A) and later progression
of seizure (B) [Spinosa2011]

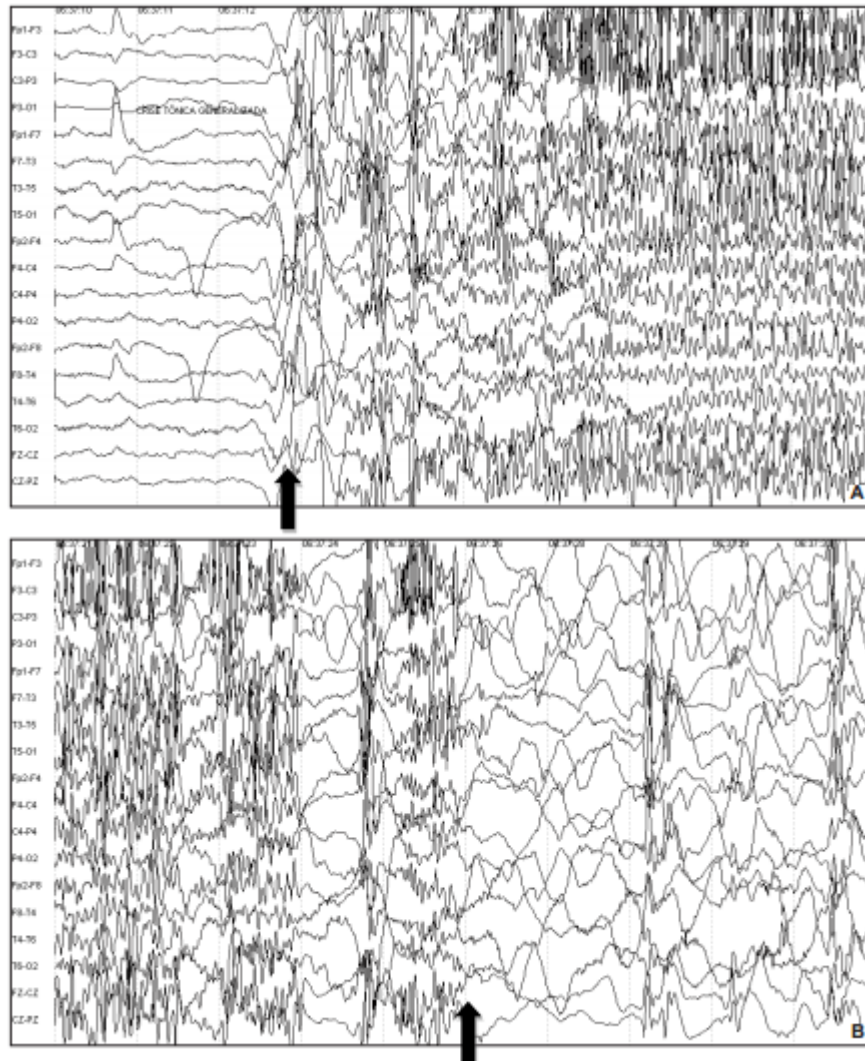


FIGURE 3.4: EEG of a generalized seizure from paediatric patient B. Beginning of seizure marked with arrow (A) and (B) end of seizure marked with arrow. [Spinosa2011]



FIGURE 3.5: EEG of a absence seizure from paediatric patient C. [Spinosa2011]

3.3 Non Linear Brain Dynamics

Evoked potentials (EPs) are time-locked electromagnetic responses in the brain following the presentation of discrete stimuli such as light flashes, audio tones and touch - the evoked EEG pattern is locked in time with respect to the external stimulation. The scalp surface measurements of such responses are on the order of a few microvolts, and as such are considered to be independently buried within the ongoing background EEG which itself has an average amplitude of a few hundred microvolts. therefore the simple model is often used to roughly represent the relationship between the EEG and the EP is

$$y(t) = s(t) + n(t)$$

where $y(t)$ is the potential recorded from the surface of the scalp, $s(t)$ is the independent EP, and $n(t)$ is the background EEG ‘noise’. The usual procedure that is followed to extract the the EP is to average the signal recorded over many stimulations (trials), such that all time-locked EEG activity will be enhanced, while non time-locked EEG activity will diminish. This method is based on the following assumptions:

1. The true underlying EP $s(t)$ is invariant between trials.
2. The neural circuitry that generates the EP is completely independent of the circuitry that generates the background EEG.
3. The ongoing background EEG is stationary between trials.
4. The current EP is not influenced by the previous EP.

However, in humans it is well known that EPs do vary between trials, and that the EEG is not neither stationary nor completely independent from the process that generates the EPs. Also the independence of the generation mechanisms of the two processes has never been proved extensively. Similarly abnormal neural activity such as epileptic seizures cannot be linearly separated from the background EEG.

Therefore a new hypothesis is needed to model the generation of EPs and other significant brain events. One such hypothesis is that the ongoing EEG experiences a reorganization that can be modelled via the non linear transformation

$$y(t) = f[e(t)] + n(t)$$

$y(t)$ is the potential recorded from the surface of the scalp, $e(t)$ is the ongoing EEG up to the neural event $n(t)$ is any non event related activity, and $f[.]$ is the non linear transformation function [Brandt2001]. Analysis of these non linear transformation functions is a currently active area of research. Clear evidence of non linearity can be easily found in the EEG by the fact that the EEG under periodic photic or auditory stimulation shows not only the frequency of stimulation but also harmonics and sub harmonics of that frequency. This is in line with the fact that a non linear dynamic system driven by a periodic frequency will not only have an output at the driving frequency but also at its harmonics and sub harmonics. [Fell2000]. Thus non linear dynamics have been increasingly used to reveal aspects of the EEG that are not visible under linear methods.

3.4 Dynamical systems

A dynamical system is a model which describes the evolution of a system given only the initial state, which gives the impression that these systems possess memory. The next state of the system is a function of the present state. Therefore a dynamical system is described by two parameters, a state - which is all the values of the variables that describe the system at a certain snapshot in time, and the dynamics of the system - a set of laws or equations which govern the evolution of the system with time.

The state of system that is described by m variables can be represented by a point in m dimensional space which known as phase space or state space. The set of equations which govern the dynamical system usually consist of a set of coupled differential equations (one for each of the systems variables) which map

the transition of the system in m dimensional space. Therefore given a m dimensional state of a dynamical system x_n^m , the next state of the system is given by:

$$\vec{x}_{n+1} = f(\vec{x}_n)$$

where $f : \mathbb{R}^m \rightarrow \mathbb{R}^m$ is a map from m dimensional space to m dimensional space. The line connection the points in m dimensional space representing the set of states reached by the system is known as the trajectory of the system.

3.5 Phase Space

Phase space, also known as state space is defined as the set of all states that can be reached by the system in question, it might be described as the living space of the dynamical system. Phase spaces are usually differentiable manifolds and thus can be treated as Euclidean spaces \mathbb{R}^n . The flow Φ on the manifold is generated by the map that transforms the initial state x_n to the subsequent state x_{n+1} .

Considering a point x of manifold M in \mathbb{R}^n phase space, if a copy of \mathbb{R}^n is attached tangentially at x the resulting space is known as tangential space. The derivative of any trajectory passing through x is a vector of the tangential space.

3.6 Attractors

If a dynamical system is observed for a sufficiently long time, i.e. until the initial transients have died out, its trajectory will converge to a subspace of the phase space. The geometric object of the subspace is known as the attractor of the system. The attractor is so called, because it attracts trajectories from all initial conditions of the system.

An attractor can be formally described as follows.

1. A set of states A is an attractor, if for a map f acting on A generating a flow Φ , $\Phi(A) \subset A$, which means that states within A will remain in A .
2. A has a neighbourhood known as the basin of attraction U such that $f(U) \subset U$ and $\bigcap_{i>0} \Phi^i(U) = A$. i.e. points within U are attracted to A
3. For conditions 1. and 2. to be fulfilled $\bar{A} \not\subset A$ i.e. A is the smallest set for which conditions 1. and 2. hold.

A linear dynamical system has only one type of attractor, a single point in phase space. This implies that the system will converge to a steady state after a certain settling time. Non linear systems have a far more varying repertoire of attractor structures. There are of three main types:

1. Limit Cycles - these are closed loops in phase space representing periodic motion.
2. k-tori - these attractors have a toroidal surface in an integer dimension, representing quasi-periodic motion with the superposition of an integer number of indecomposable frequencies.
3. Chaotic or strange attractors - this a very complex object with what is known as 'fractal geometry'. The dynamics of chaotic or strange attractors correspond to deterministic chaos.

Figure 3.6 illustrates the different types of attractors.

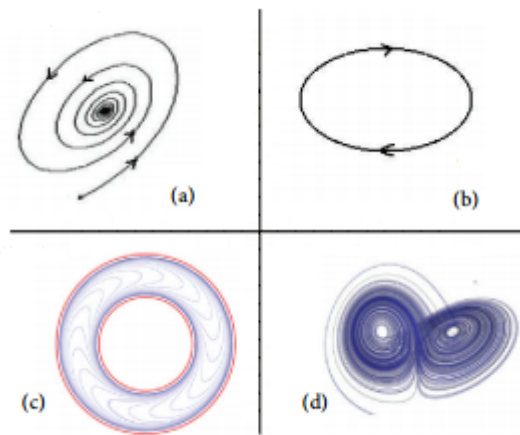


FIGURE 3.6: Four different types of attractors, (a) a point attractor, (b) a limit cycle, (c) a torus, (d) a strange attractor

Deterministic chaos is a type of dynamics that is deterministic while at the same time is seemingly random. As such chaotic dynamics can be predicted only for a short amount of time. A characteristic of a chaotic attractor is that it never repeats the same state, even though it is confined to the attractor subspace.

3.7 Characterisation of attractors - Lyapunov Exponents

Lyapunov exponents indicate the exponential divergence or convergence of nearby trajectories of an attractor due to small perturbations in initial conditions. Considering an initial state x_0 with a small perturbation δ_0 after n states,

$$x_0 + \delta_0 \rightarrow x_n + \delta_n \tag{3.1}$$

Considering a single dimensional discrete system with a map $f(\cdot)$, the following exponential evolution of the perturbation δ can be assumed:

$$\delta_n = \delta_0 e^{\lambda n} \quad (3.2)$$

then

$$\lambda = \frac{1}{n} \ln \left(\frac{\delta_n}{\delta_0} \right) \quad (3.3)$$

$\delta_n = f^n(x_0 + \delta_0) - f^n(x_0)$ where x_0 is the n-times application of $f(\cdot)$. Then

$$\lambda = \frac{1}{n} \ln \left(\frac{f^n(x_0 + \delta_0) - f^n(x_0)}{\delta_0} \right) \quad (3.4)$$

$$\lambda = \frac{1}{n} \ln \left(\frac{d(f^n)(x_0)}{dx} \right) \quad (3.5)$$

The Lyapunov exponent is then defined as the upper limit for $n \rightarrow \infty$ for the above equation.

$$\lambda(x_0) = \limsup_{n \rightarrow \infty} \frac{1}{n} \ln \left(\frac{d(f^n)(x_0)}{dx} \right) \quad (3.6)$$

A system will have as many Lyapunov exponents as there are dimensions in its phase space. A positive Lyapunov exponent indicates that the attractor will diverge, while a negative Lyapunov exponent will indicate that the attractor will converge. The largest Lyapunov exponent of an attractor describes the expansion along the principle axis of the attractor hypercube over a given time interval. If the largest Lyapunov exponent is greater than zero, the system will show sensitivity to the initial conditions. i.e. chaos.

The concept of entropy which is defined as the rate of information loss over time, is equal to the sum of all positive Lyapunov exponents [**Stam2005**]

3.8 Embedding - Attractor Reconstruction

A dynamical system may have a three dimensional attractor but only one dimension of it may be measurable as a time series. Thus the purpose of embedding is to recreate the m -dimensional attractor from a single visible time series. The embedding is then a representation of the original attractor in its phase space. Therefore mathematically speaking the embedding of an object A is a diffeomorphic map of A into another phase space. This means that there is a bijection from the true attractor to the embedding. According to the weak Whitney embedding theorem, any smooth real manifold in d dimensional space can be embedded in m dimensional space given that $m > 2d$. Therefore for a smooth manifold A in m dimensional space, any smooth map $\mathbb{R}^d \rightarrow \mathbb{R}^{2d+1}$ is an embedding of A . In simple words this means that if $2d + 1$ dimensions are used, an embedding is guaranteed. The work of Takens [Takens1981] deals with the process of creating the embedding from a single observable time series. According to Takens, if f is a smooth map acting on an m dimensional manifold M , generating a flow Φ , which in turn generates a measurement y an embedding $E_{f,y} : M \rightarrow \mathbb{R}^m$ is given by:

$$E_{f,y}(\tilde{x}) = (y(\Phi_0(x)), y(\Phi_\tau(x)), y(\Phi_{2\tau}(x)), \dots, y(\Phi_{m\tau}(x))) \quad (3.7)$$

The $2m$ components of the state vectors \tilde{x} in the embedding space are simply the measured values of y_t that are shifted in time by a time delay. τ i.e.

$$\tilde{x}_0 = (y_t, y_{t+\tau}, y_{t+2\tau}, \dots, y_{t+m\tau}) \quad (3.8)$$

By the repetition of this procedure for the next m set of delayed values we obtain the vector of the next state in the embedded space.

$$\tilde{x}_1 = (y_{t+1}, y_{t+1+\tau}, y_{t+1+2\tau}, \dots, y_{t+1+m\tau}) \quad (3.9)$$

The proper choice of both τ and $m > 2d + 1$ is important but difficult step in non linear analysis since these two parameters need to be estimated from a single time series. According to Takens, nearly every value of τ will give a correct embedding. However there are practical reasons behind the proper choice of τ . A value of τ that is too small will make $\Phi_{k\tau}(x) \cong \Phi_{k\tau}(x)$ causing the attractor to be compressed in the diagonal of the embedding space. If the value of τ is too large $\Phi_{k\tau}(x)$ and $\Phi_{k\tau}(x)$ will become dynamically unrelated causing the attractor structure to disappear. Several methods exist for the determination of optimal embedding parameters in which the optimum time delay τ_{opt} and the optimum number of embedding dimensions m_{opt} are found separately. Usually τ_{opt} is found first by determining for which value of τ the mutual information between samples x_k and $x_{k+\tau}$ is minimum [Fraser1986]. m_{opt} is found next usually by calculating the number of false nearest neighbours between embeddings when the number of embedding dimensions is increased from m to $m + 1$. m_{opt} is found at the point where the number of false nearest neighbours is minimum [Kennel1992].

3.9 Optimum Embedding Parameter Estimation

Gautama et al. [Gautama2003] presented a method of jointly estimating the optimum embedding parameters τ_{opt} and m_{opt} based on the Kozachenko-Leonenko (K-L) estimate of the differential entropy [Beirlant1997]. Differential entropy is an extension of Shannon entropy to continuous probability distributions. The

differential entropy is given by

$$H(x) = - \int_{-\infty}^{+\infty} p(x) \ln p(x) d(x)$$

The K-L estimate of differential entropy is given by:

$$H(x) = \sum_{j=1}^N \ln(N\rho_j) + \ln 2 + C_E \quad (3.10)$$

In the above equation N is the number of samples in the data set. ρ_j is the Euclidean distance of the j^{th} delay vector to its nearest neighbour and C_E is the Euler–Mascheroni constant ≈ 0.5772 . The method of Gautama et al. is to estimate $H(x, m, \tau)$ for a given time series x with embedding parameters m and τ . and then minimise $H(x, m, \tau)$ such that

$$\min H(x, m, \tau) = H(x, m_{opt}, \tau_{opt})$$

The K-L differential entropy estimate is not robust with respect to changes in dimensionality. Therefore, ‘surrogate’ time series of the signal x , x_{s_i} where $i = 1, \dots, N_s$ are generated performing random permutations of the time series. This yields a whitened signal with a distribution identical to the original signal. The K-L differential entropy estimates for both the original and surrogate time series are calculated for increasing values of m and τ . The optimum embedding parameters are then calculated by minimising the ratio

$$I(m, \tau) = \frac{H(x, m, \tau)}{\langle H(x_{s_i}, m, \tau) \rangle} \quad (3.11)$$

where $\langle \cdot \rangle$ denotes the average over i .

3.10 Non Linear Analysis of the Epileptic Seizures

A complex non linear system may have more than a single type of attractor. During the evolution of time, small perturbations in the parameters that govern the system may drastically change the trajectory of the system in phase space. The transition from one type of attractor to another may not happen abruptly, but may 'flicker' between basins of attraction [Dakos2013]. Transitions from interictal EEG activity to ictal activity often follow such intermittent behaviour. There are only a small number of parameters that can cause a dynamical system to completely change its structure so as to cause a transition to another type of attractor, i.e. a bifurcation. Thus a bifurcation represents a qualitative change that depends on a small set of critical parameters that define the operating characteristics of a dynamical system. An epileptic seizure may occur due to a change in some critical parameters of a neuronal network which cause a bifurcation to a different attractor. The dynamics of seizure generation were reviewed by Lopes da Silva et al. [LopesdaSilva2003], who proposed three different scenarios.

1. Sudden emergence of a seizure out of normal background activity. A separatrix (a plane of separation) exists between two clearly defined basins of attraction. The dynamics of such systems show hysteresis where the systems dynamics abruptly jump from one oscillatory mode to another.
2. Reflex epilepsy: the transition to another attractor due to an external stimulus such as flickering light. These stimulations cause resonance at harmonic and sub harmonic frequencies of the stimulus in the neural networks of the brain. A mechanical analogy of this could be the

synchronizations of the pendulums of two mechanical clocks hung on the same wall.

3. Gradual transition from normal to seizure activity through a series of bifurcations. - The distance between between the basin of attraction of normal behaviour and the separatrix gradually diminishes. Usually there is enough of a gap between the two basins of attraction, that small perturbations in the normal attractor fall back into the basin of attraction. However as the distance between the two basins diminishes, a transition to a seizure eventually occurs.

Chapter 4

Methodology

4.1 Epoching of EEG Data

Epoching is the process of extracting time windows of a specific length from the continuous EEG signal. Considering prior research on the criticality of EEG Epoch length we can turn to that of Levy [Levy1987]. Levy studied the effect of epoch length on the power spectrum of the EEG and concluded that 2 second long epochs identified changes in the EEG more rapidly than longer epoch length. The slicing of the continuous EEG stream into finite epochs can however introduce contamination of the spectra created by the spectral leakage caused by the abrupt transitions at the end of the epoch. This is usually corrected by the windowing process during spectral estimation. However, applying windows causes a loss of amplitude at the beginning and end of the epochs. This can be compensated for by causing the epochs to overlap usually at 50% of the epoch.

4.2 Preprocessing of EEG Data

Prior to the analysis, EEG signals in their raw form need preprocessing. Preprocessing of the EEG often includes filtering and artefact removal since recordings can contain noise that is mixed in the electrical activity of the brain.

Power line noise at 50 or 60 Hz, electrode noise, eye blinks and movement of the sensors due to facial muscles, which in turn cause electromyogenic artefacts all tend to corrupt the EEG. A notch filter is usually used to filter out power line noise, however there has been little justification to use such high frequencies in EEG analysis because most brain activity occurs between 3 and 29 Hz [Fergus2015]. Libenson [Libenson2009] has also argued that most EEG instruments rarely exceed 30 - 40 Hz and recordings from cortically implanted electrodes 50 Hz due to electrical noise and muscle artefacts. Greene et al. [Greene2008] state that the frequency range between 2 - 20 Hz provide the best discrimination between seizure and non seizure events. Considering the lower cut-off frequency of EEG data Libenson again argues that there is no cerebral activity below 0.5 Hz. In light of these reports the preprocessor filtering range for the EEG was chosen to be 0.5 - 30 Hz.

4.3 Smoothed EEG Subtraction

It is quite evident that the spikes and other deformities in the EEG signal carry significant information about abnormal behaviour in the brain, when compared to the baseline oscillations of the neural networks. Such sudden spikes and abnormalities will often indicate bifurcations in the non linear dynamics of the brain [Rodrigues2009]. Thus drawing inspiration from the method of Altunay et al. [Altunay2010] Smoothed EEG Subtraction is used to extract these spikes and other abnormalities and deformities from the original EEG signal. Feuerstein et al. [Feuerstein2009] have shown how Savitzky-Golay filtering can be used to remove unwanted spikes from data measurements, however, in this method the reverse is necessary spikes and abnormalities are required while the baseline EEG signal is not. Thus a 2nd order Savitzki -

Golay Filter with a window width of 5 samples is used to smooth the EEG signal from each EEG channel. The smoothed EEG data is then subtracted from the original EEG data.

4.4 EEG Channel Fusion

The EEG contains data from multiple channels recorded from different areas of the brain, and epileptic seizures usually originate from the same areas of the brain for a given patient. However this not always the case and as such excluding EEG channels where seizure activity does not occur is not a wise choice. Therefore a method is presented to fuse the data in all the EEG channels based on the FFT approximation method of Lehmann and Michel [Lehmann1990], the Global Field Power [Lehmann1980] and the Stockwell Transform [Stockwell1996].

4.4.1 The FFT Approximation Method of Lehmann and Michel

This method assumes that there is a single dipole generator for every single frequency in the EEG and then localizes the multichannel EEG to that single dipole. The process begins with taking the FFT of each channel of each EEG epoch and then plotting the sine cosine diagrams for all the channels at each frequency point of the FFT. This results in a unique constellation diagram that describes the electric field distribution at each frequency point in the EEG.

The single dipole is approximated on the sine - cosine map by taking the best fit straight line through the origin (the mean value of all entries) which gives the least sum of squared deviations from the original entries in the map and their corresponding projections onto the straight line.

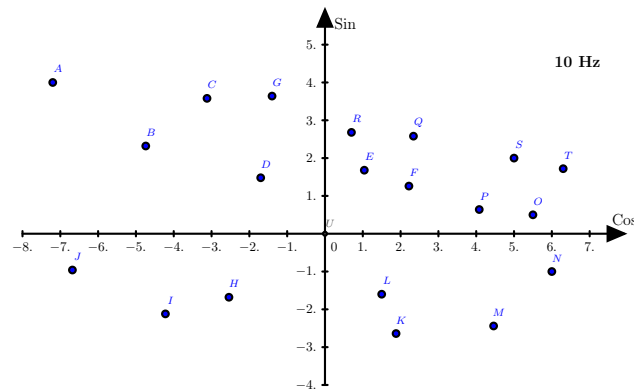


FIGURE 4.1: Sine - Cosine plot

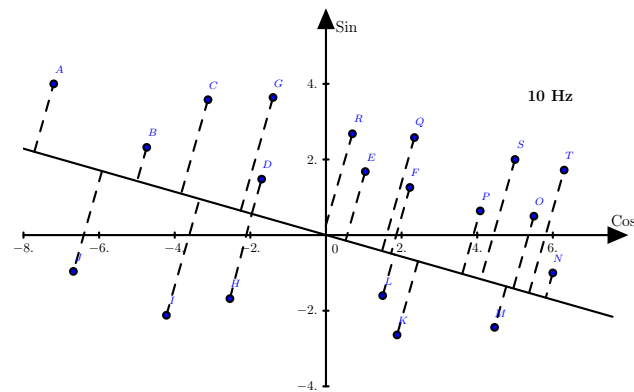


FIGURE 4.2: Orthogonal projections onto the single dipole FFT approximation line

The projections above the line are considered to be positive while the projections below the line are considered to be negative. The length of the projections gives the contribution from the respective EEG channel to the single frequency dipole.

4.4.2 Global Field Power

Global field power [Lehmann1980] is a measure that allows one to quantify the quantify the electrical activity in each sine - cosine map by computing a type of spacial standard deviation. The rationale behind this idea is that certain channels presumably contain little information, while certain channels

contain maximal information about the electrical activity at that frequency, reflecting the synchronous activation of a large number of neurons. Global field power is used to quantify this activity and is calculated as the standard deviation of the length of all orthogonal projections onto the single dipole FFT approximation line.

The method of Lehmann and Michel assumes that the EEG is stationary across individual epochs. However as it now well known that the EEG is non stationary, and therefore the time-frequency distribution via the Stockwell transform is used for the FFT approximation process.

4.4.3 The Stockwell Transform

The Stockwell transform [Stockwell1996] is a time - frequency decomposition that synchronously probes both the local amplitude and the power spectrum of a time series. The Stockwell transform $S_x(\tau, f)$ for a time series $x(t)$ is calculated as:

$$S_x(\tau, f) = e^{i2\pi f\tau} W_x(\tau, d) \quad (4.1)$$

where $W_x(\tau, d)$ is the wavelet transform of the signal $x(t)$

$$W_x(\tau, d) = \int_{-\infty}^{+\infty} x(t) w(t - \tau, d) dt$$

the mother wavelet $w(t, f)$ is given by:

$$w(t, f) = \frac{|f|}{\sqrt{2\pi}} e^{-\frac{t^2 f^2}{2}} e^{-i2\pi ft}$$

the factor d is the inverse of the frequency f . thus the Stockwell transform is given by:

$$S_x(\tau, f) = \frac{|f|}{\sqrt{2\pi}} \int_{-\infty}^{+\infty} e^{-\frac{t^2 f^2}{2}} e^{-i2\pi f t} dt \quad (4.2)$$

The width of the Gaussian window in the above equation is determined by the inverse of the frequency f . Thus the window provides good frequency resolution at lower frequencies, and good time resolutions at higher frequencies. This was compensated for by Assous and Boashash [Assous2012] by introducing two new parameters m and k which are used to control the width and variance of the Gaussian window to appropriately localize the low and high frequencies of the Stockwell transform. The now modified Stockwell transform is given by:

$$S_x(\tau, f, m, k) = \frac{|f|}{(mf + k)\sqrt{2\pi}} \int_{-\infty}^{+\infty} e^{-\frac{t^2 f^2}{2(mf+k)^2}} e^{-i2\pi f t} dt \quad (4.3)$$

The parameter k is selected as $\frac{1}{N}$, where N is the length of the sequence $x(t)$. The parameter m is four times the variance of the sequence $x(t)$.

The EEG channels are fused as follows. The Stockwell transform for each channel of each EEG epoch is calculated resulting in a $T \times F \times M$ three dimensional matrix where T is the number of time steps, F is the number of frequency steps and M is the number of EEG channels. From this an $F \times M$ sub matrix is extracted for each time step $t \in T$. Each element of a given row vector in this matrix gives the contribution of an EEG channel to the frequency point represented by the said row vector.

The Global field power is then calculated using the method given above for each row in the $F \times M$, giving a column vector of length F for each time step $t \in T$.

This results in a $F \times T$ matrix containing the fused time-frequency representation of the EEG epoch. Finally the inverse Stockwell transform is used to regenerate a time series representing the entire EEG epoch.

4.5 Identification Of Changes in Optimum Embedding Parameters

From the work of Lopez da Silva [**LopesdaSilva2003**] it can be seen that there is a change in the structure of the attractor of the EEG during an epileptic seizure. Therefore this method now attempts to detect a seizure by looking for sudden changes in the optimum embedding parameters of the time series obtained by fusing the multichannel EEG. Using the method outlined by Gautama et al. [**Gautama2003**] the optimum embedding parameters for each fused EEG epoch are calculated and plotted with respect to time. A sudden bifurcation of the attractor should be indicated by a change in the optimum embedding dimension showing that a sudden change in the dynamics of the neural networks of the brain has occurred.

Chapter 5

Materials and Testing

5.1 The EEG Data Set

Scalp EEG data from 10 paediatric patients, taken from the CHB-MIT EEG database [Goldberger2000] was used to evaluate the performance of the previously described method for the detection of epileptic seizures. The EEG was recorded at the Children's Hospital, Boston USA from children undergoing withdrawal from epilepsy medication in preparation for brain surgery. The EEG was recorded at a sampling rate of 256 Hz, using a 20-channel 10-20 bipolar montage. The seizures that have been recorded are clinical seizures, i.e. physical manifestations of the seizure are visible, as opposed to sub-clinical seizures where there are no physical signs of the seizure but the EEG record shows signs of an ongoing seizure [Bromfield2006]. The EEG data has been segmented into seizure and non seizure records that are usually one hour in length. 10 hours of seizure and non seizure records are selected from each patient taking into account as many seizures as possible from each patient. The 10 patients were selected such that seizure records from each patient had only one seizure per seizure record. Records longer than one hour were segmented into hour long records.

5.2 Preliminary Testing Of The Proposed Method

The Proposed method given in chapter 4 was tested using MATLAB 2015a (The MathWorks, Inc.) in conjunction with EEGLAB, an open source toolbox for analysis of single-trial EEG dynamics [Delorme2004].

5.3 Detecting Changes in Optimum Embedding Parameters - Preliminary Tests

The change in number of optimum embedding dimensions m_{opt} with respect to the emergence of an epileptic seizure were first tested on a preliminary basis on three patients taking one seizure record and one non seizure record from each of the patients. Data from patients 3, 5 and 9 were randomly chosen for this test.

5.3.1 Results From Patient No. 3 - Seizure record

Figure 5.1 shows the changes in the value of m_{opt} that were calculated for EEG record number 1, in which a seizure is observed to have occurred at 362 seconds into the record. The value of m_{opt} for the system oscillates between 4 and 6 dimensions during the preictal state, indicating that the EEG has a fractal nature. However at 362 seconds m_{opt} rises to 8 dimensions, drops to 7 dimensions at 364 seconds and then moves between 8 and 9 dimensions before returning to 6 dimensions at 404 seconds. It then gradually settles down to 4 dimensions at 414 seconds. There are also a few high dimensional spikes around 950 seconds as well as another prominent one at 2592 seconds. There are also a few negative going spikes indicating a sporadic decrease in the number of optimum embedding

dimensions. Figure 5.2 shows a zoom up of the area of the seizure depicted in Figure 5.1.

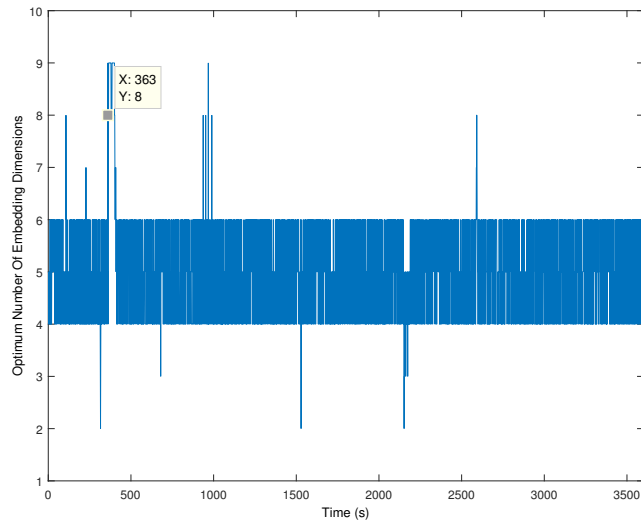


FIGURE 5.1: Optimum embedding dimension, patient 3, record no. 1

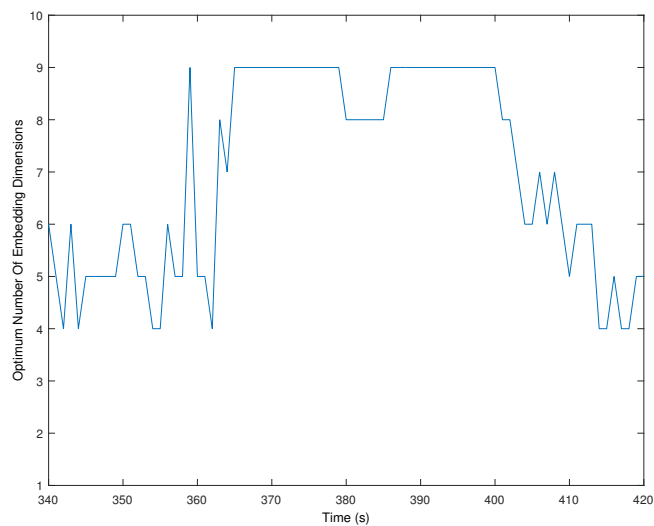


FIGURE 5.2: Zoom in to seizure occurring in figure 5.1

Looking at the EEG that generated the above figures, the sudden onset of the seizure can be clearly seen in Figure 5.3.

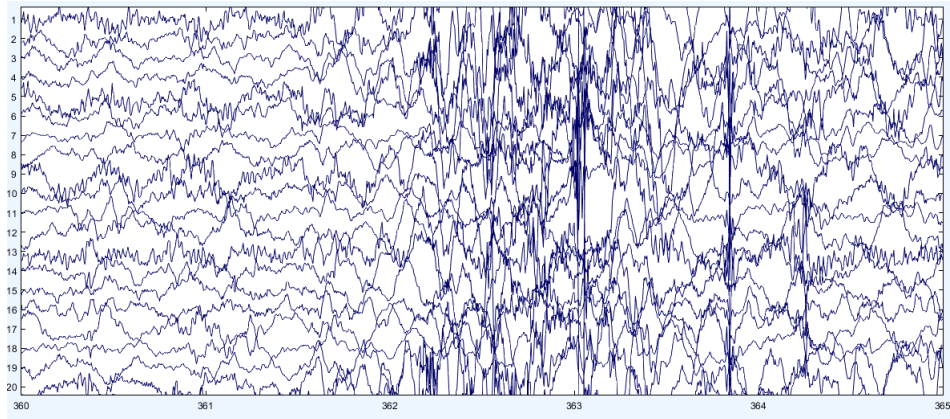


FIGURE 5.3: EEG at start of seizure, patient 3, record no. 1

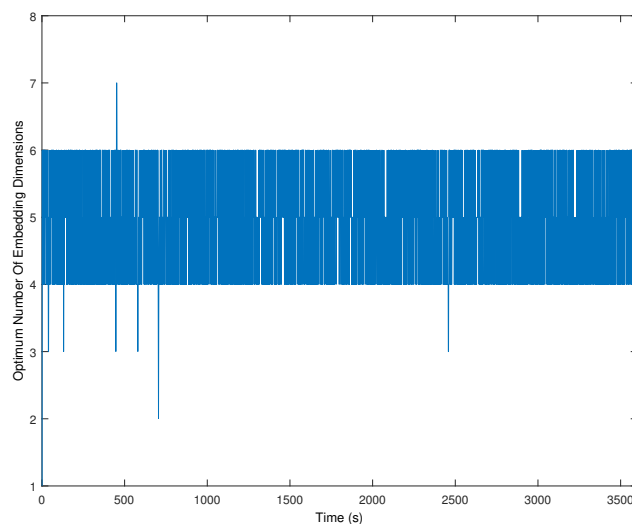


FIGURE 5.4: Optimum embedding dimension, patient 3, record no. 14

5.3.2 Results From Patient No. 3 - Non Seizure record

Figure 5.4 shows the changes in the changes in the value of m_{opt} that were calculated for EEG record number 14, in which a seizure does not occur.. The system's m_{opt} again oscillates between 4 and 6 dimensions during the preictal

state. Small positive going and negative going spikes randomly occur indicating a sporadic increase and decrease in the optimum number of embedding dimensions.

5.3.3 Results From Patient No. 5 - Seizure record

Figure 5.5 shows the changes in the changes in the value of m_{opt} that were calculated for EEG record number 17, in which a seizure is observed to have occurred at 2451 seconds into the record. The system in this patient's record oscillates between 2 and 4 optimum dimensions during the preictal state, also indicating that the EEG has a fractal nature. However beginning at 2447 seconds the value of m_{opt} slowly rises to 12, and continues to oscillate between 10 and 12 dimensions until 2572 seconds. It then moves between 8 and 10 dimensions until briefly returning to the values it had during its preictal state at 2630 seconds. the value of m_{opt} again rises slightly and oscillates between 4 and 6 dimensions before finally setting down to between 2 and 4 dimensions as 2740 seconds. Notable spikes are also visible at 3197 seconds and 3521 seconds.

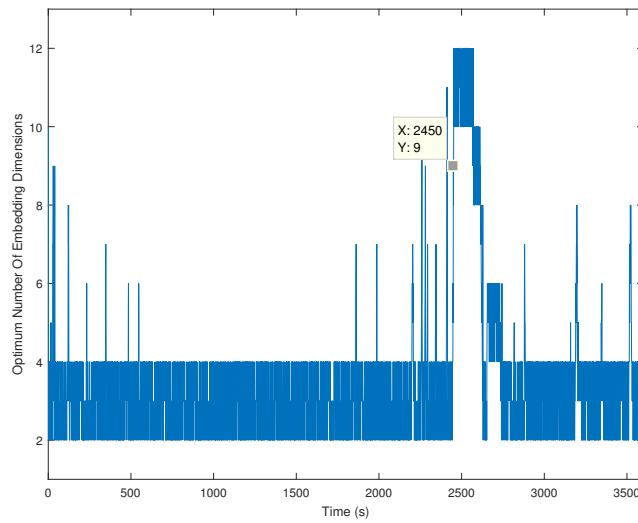


FIGURE 5.5: Optimum embedding dimension, patient 5, record no. 17

A zoom in of the change in m_{opt} for Figure 5.5 is shown in Figure 5.6

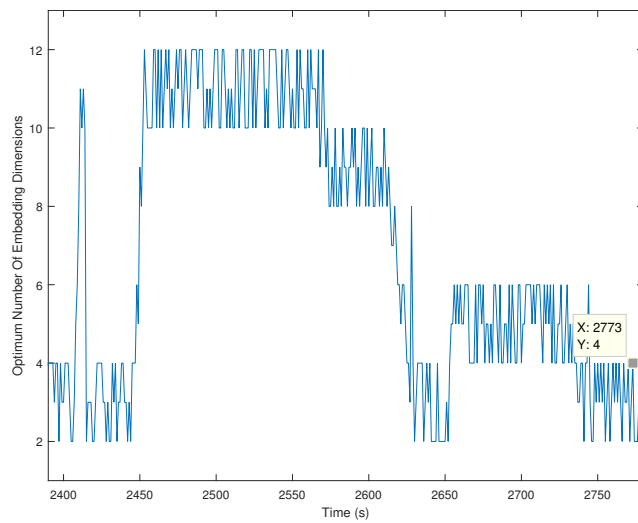


FIGURE 5.6: Zoom in to seizure occurring in figure 5.5

Considering the actual EEG that generated Figures 5.5 and 5.6, Figure 5.7 shows the start of typical spike and wave EEG pattern beginning at 2152 seconds.

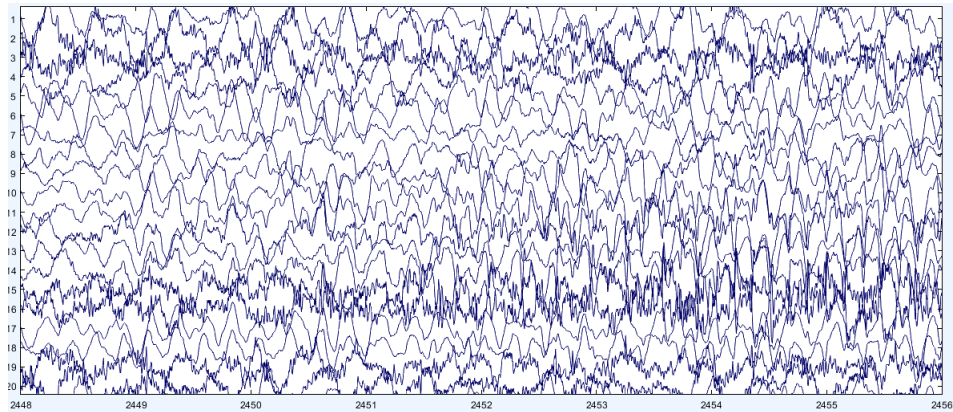


FIGURE 5.7: EEG at start of seizure, patient 5, record no. 17

Considering the oscillation of m_{opt} between 2650 seconds and 2740 seconds as shown in Figure 5.6, the EEG in Figure 5.8 shows a pulsating pattern indicative of spasms of the facial muscles caused by chewing [Shoeb2009]. However this EEG pattern is reminiscent of a seizure with superimposed muscle artefacts [Mirski2008].

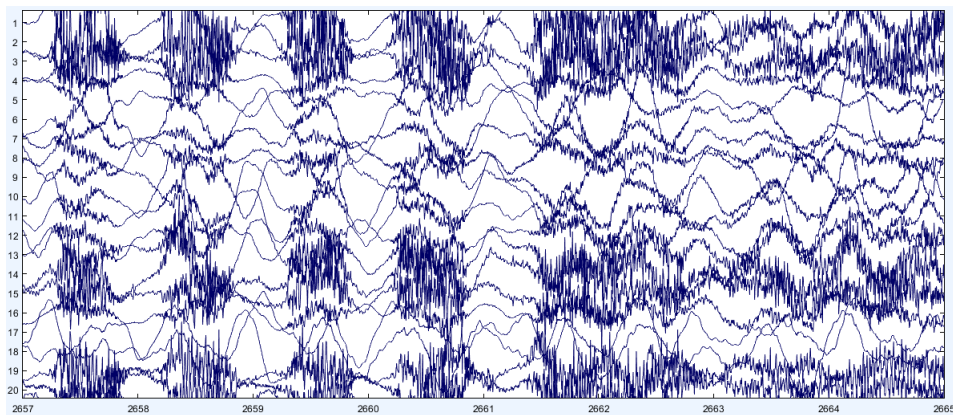


FIGURE 5.8: EEG, 2657s - 2665s, patient 5, record no. 17

Figure 5.9 shows the EEG responsible for generating the spike in the vicinity of 3197 seconds, while Figure 5.10 shows the EEG responsible for generating the spike in the vicinity of 3521 seconds.

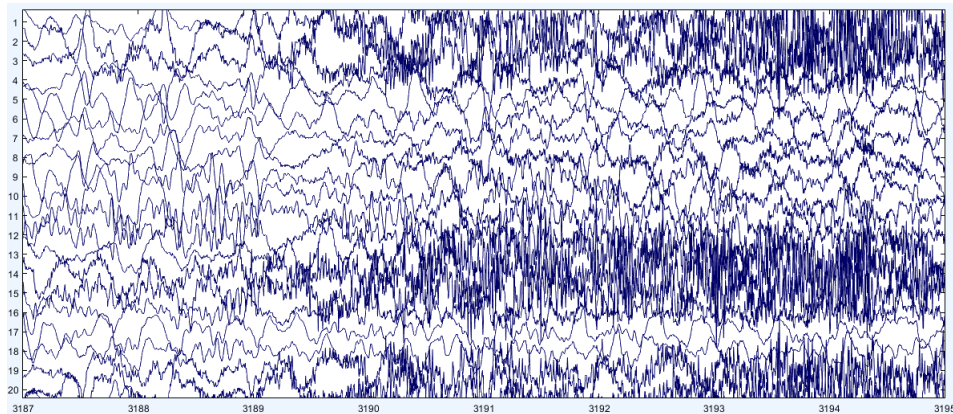


FIGURE 5.9: EEG, 3187s - 3195s, patient 5, record no. 17

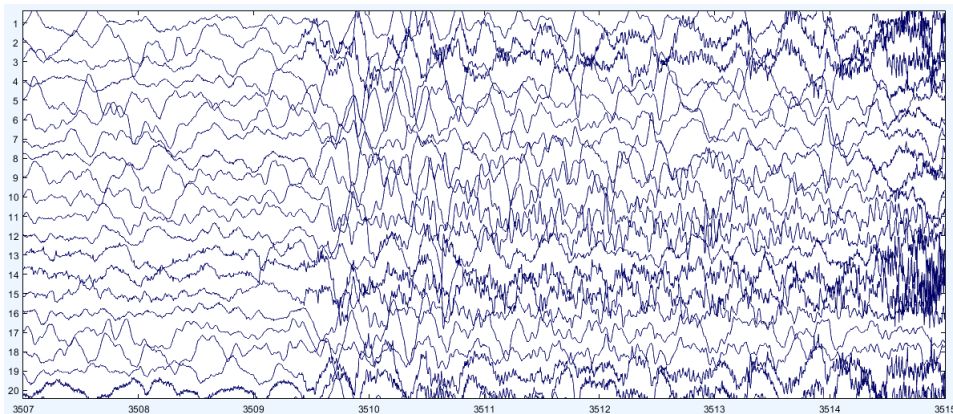


FIGURE 5.10: EEG, 3507s - 3515s, patient 5, record no. 17

5.3.4 Results From Patient No. 5 - Non Seizure record

Figure 5.11 shows the changes in the value of m_{opt} that were calculated for EEG record number 4, in which a seizure does not occur. The system's m_{opt} again oscillates between 2 and 4 dimensions during the preictal state. Small positive going and negative going spikes randomly occur indicating a sporadic increase and decrease in the optimum number of embedding dimensions.

The main feature though is the indication of a seizure which begins at 2809 seconds.

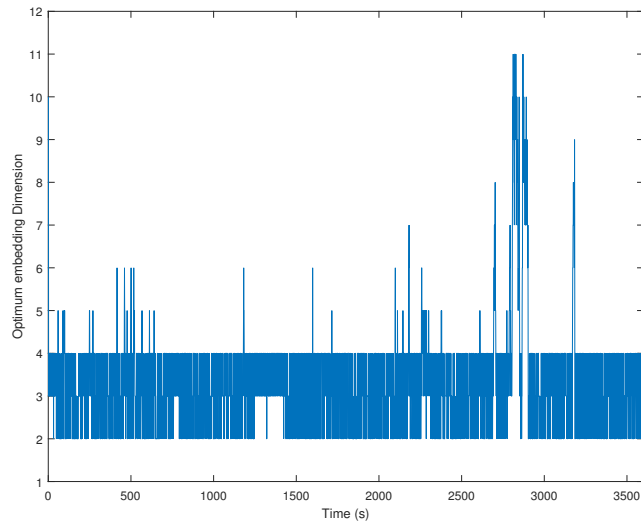


FIGURE 5.11: Optimum embedding dimension, patient 5, record no. 4

A further zoom in of the area around the indicated seizure is shown in figure 5.12.

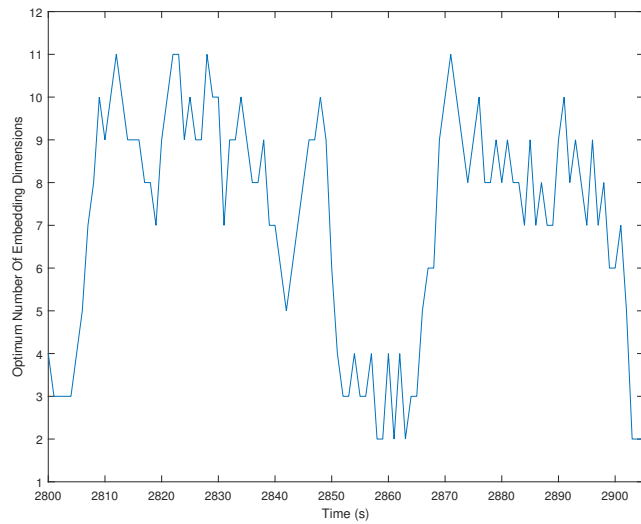


FIGURE 5.12: Zoom in of unexpected seizure in figure 5.11

Looking at the EEG of the time period depicted in Figure 5.12, the pattern presented in Figure 5.13 resembles a burst suppression pattern of a *non convulsive status epilepticus* as described by Sutter and Kaplan [Sutter2012].

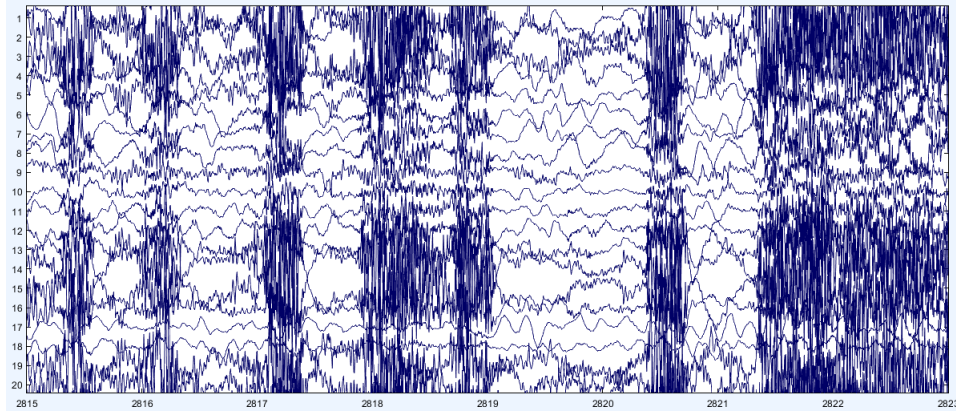


FIGURE 5.13: EEG, 2815s - 2823s, patient 5, record no. 17

5.3.5 Results From Patient No. 9 - Seizure record

Figure 5.14 shows the changes in the changes in the value of m_{opt} that were calculated for EEG record number 8, in which a seizure is observed to have occurred at 3021 seconds into the record. The system in this patient's record oscillates between 4 and 5 optimum dimensions during the preictal state, with random drops down to 3 optimum dimensions. Beginning at 2957 seconds the value of m_{opt} slowly rises to 11, and continues to oscillate between 8 and 11 dimensions until 3031 seconds. It then moves between 5 and 8 dimensions until 3241 seconds. The system then continues to move between 4 and 6 optimum dimensions with random drops to 3 optimum dimensions until the end of the record. Figure 5.14 zooms into the area where the seizure occurs in Figure 5.15.

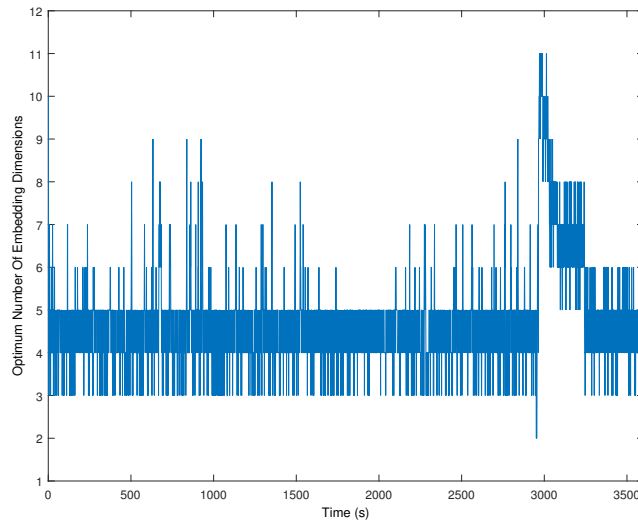


FIGURE 5.14: Optimum embedding dimension, patient 9, record no. 8

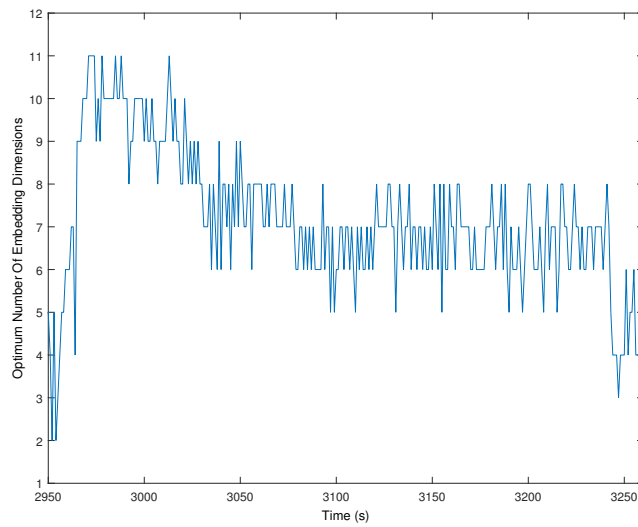


FIGURE 5.15: Zoom in to seizure occurring in figure 5.14

The EEG segments that generated the start of the seizure Figures 5.14 and 5.15 is shown in Figure 5.16.

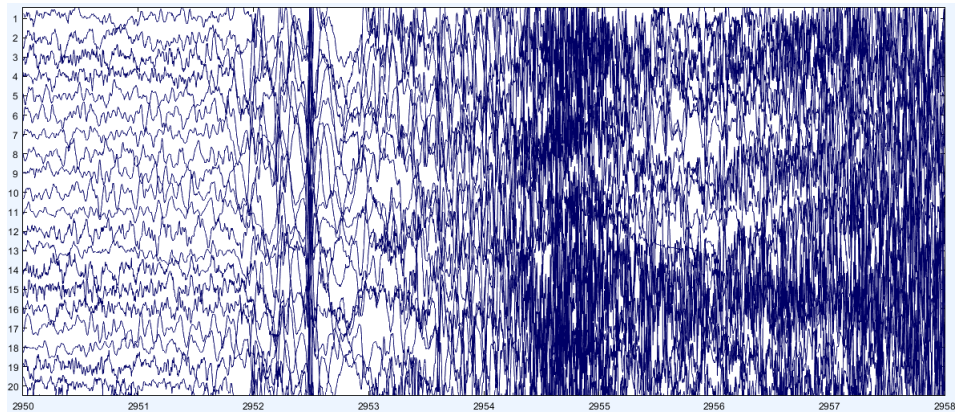


FIGURE 5.16: EEG at start of seizure, patient 9, record no. 2

5.3.6 Results From Patient No. 9 - Non Seizure record

Figure 5.17 shows the changes in the changes in the value of m_{opt} that were calculated for EEG record number 2, in which a seizure does not occur.. The system's m_{opt} again oscillates between 4 and 5 dimensions with random drops down to 3 optimum dimensions. Small positive going a spikes randomly occur indicating a sporadic increase and decrease in the optimum number of embedding dimensions.

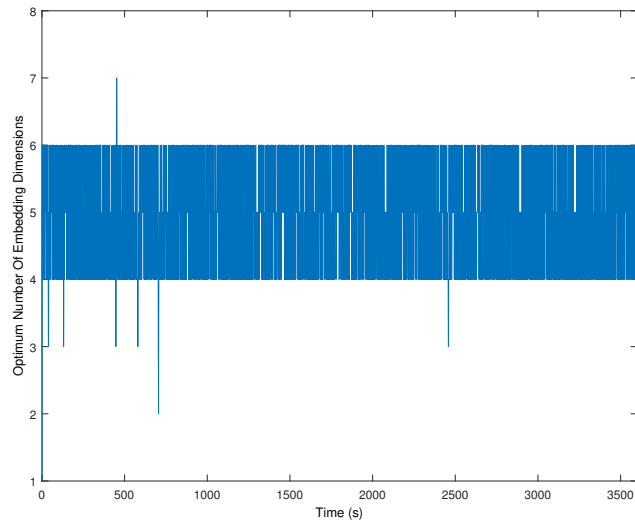


FIGURE 5.17: Optimum embedding dimension, patient 9, record no. 2

5.4 Analysis Of Preliminary Results

The following conclusions can be gleaned from the above preliminary results:

- The preictal value of m_{opt} will oscillate around a single value with usually unitary positive and negative excursions.
- When a seizure occurs, there will be a slow to sudden rise in m_{opt} .
- Sudden spikes in m_{opt} related to detection anomalies do not last more than 2 - 3 seconds.
- Non seizure records may have detections that resemble seizures but have not been classified as clinical seizures in the dataset.

5.5 Further Processing For Automatic Blind Detection of Seizures

5.5.1 Calculation Of Detection Threshold

With respect to the conclusions drawn in section 5.4, the following processing steps can now be described to obtain a threshold value for m_{opt} in order to declare a seizure.

1. Randomly choose one of the data records for a given patient from the dataset.
2. Using the method outlined in chapter 4 obtain the time series of the values of m_{opt} with respect to time.
3. Using k-means clustering with $k = 2$ obtain the two means of the clusters created.
4. Round up the higher mean value to its nearest integer, and round down the lower mean value to its nearest integer. This process isolates the preictal boundaries of m_{opt_l} and m_{opt_u} for the given patient.
5. The upper rounded value m_{opt_u} is then added to an integer M which is a control value of sensitivity is then used as the threshold $m_{opt_{th}}$. A lower value of M will increase the sensitivity of the detector, while a higher value will do the opposite. From the preliminary test data a value of $M = 3$ seems suitable for this process.

Applying the above process to the data obtained from patient 5, record 17, the two means are found to be at 4.9895 and 2.5007, rounding this data, the borders

for the preictal values m_{opt_u} and m_{opt_l} are 5 and 2 respectively. Figure 5.18 shows this, with the two red horizontal lines indicating the limits, and the green horizontal line represents $m_{opt_{th}} = m_{opt_u} + M$, where $M = 3$.

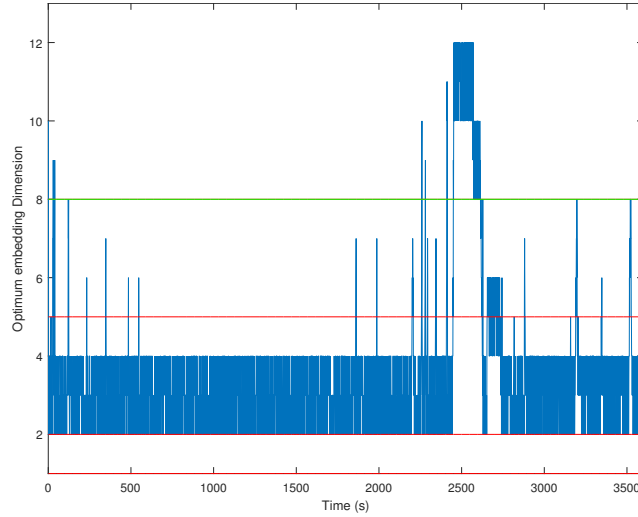


FIGURE 5.18: Application of threshold detection to record no. 14, patient 5

5.5.2 Detection Delay

From Figure 5.18 it is clear that if the threshold value of $m_{opt_{th}}$ is directly used, the detector will pick up the spurious spike that occur in m_{opt} therefore a delay of T seconds will be used in the detection process. Thus If the value of m_{opt} remains above the threshold value of $m_{opt_{th}}$ for a period greater than T seconds a seizure will be declared. A value of $T = 44$ seems a suitable value based on the preliminary test results.

5.6 Final Testing of the Proposed Method

As stated in section 5.1, 10 hours of hour long EEG records from 10 patients are used for this purpose, However the number of seizure records for each patient changes in the CHB-MIT dataset, thus all seizure records for each patient are selected, and the remaining non seizure records are selected randomly. Figure 5.19 Illustrates the distribution of seizure and non seizure records of the 10 patients used in this test.

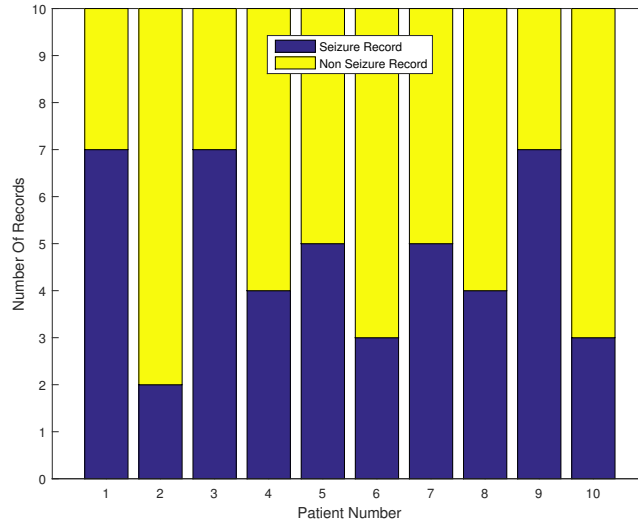


FIGURE 5.19: Distribution of seizure and non seizure records across the 10 patients

5.6.1 Performance Metrics

Two metrics will be used to characterize the performance of the proposed seizure detection method.

1. Average seizure onset detection delay via EEG D_{siez}

This refers to the delay between the stated clinical seizure onset time and the time that the seizure is declared via the scalp EEG. The indication

of the seizure in the EEG may or may not precede the onset of clinical symptoms. This is defined per patient.

2. Sensitivity S This refers to the percentage of correctly identified seizures per patient.

The number of false detections was also planned to be used, however in light of the preliminary test results it was decided not to use it as the false detections, may or may not be sub clinical seizures and there was no method at the present time to correctly differentiate between a sub clinical seizure and an EEG artefact.

5.6.2 Detector Performance

The performance of the detector was tested on a computer system based on a Intel Core i7 6800K 3.4 Ghz Hexa Core processor, 16 GB DDR 4 3000 MHz RAM and a Sapphire Radeon RX 480 Nitro+ 8GB GDDR5 GPU. The software was written with a mixture of MATLAB and C++. ViennaCL an open source scientific computing library from the Institute for Microelectronics, Vienna, Austria supporting the openCl language, was used to accelerate parts of the MATLAB code on the computers GPU, to radically speed up the computation process.

Detection Delay

Figure 5.20 illustrates the delay with which the detector declared the onset of each seizure for the ten patients in the test indicated by the 10 stem plots. While pre-detection was indicated for a few seizures, a bulk of the seizures were detected after the given seizure onset time. The mean delay with which the detector declared the seizures was 3.59 seconds.

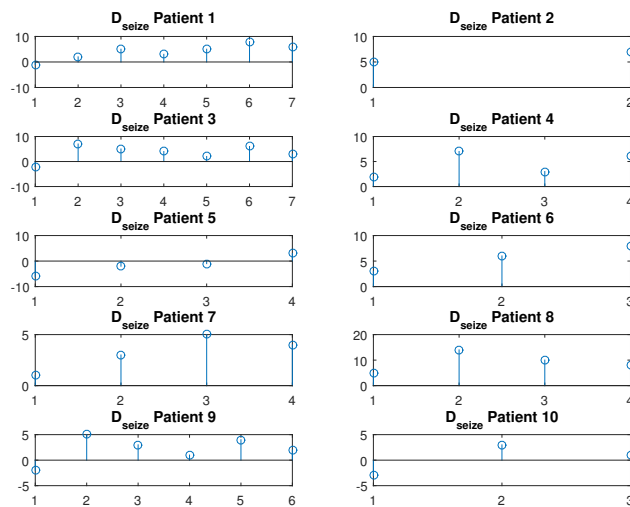


FIGURE 5.20: Seizure detection delays for the 10 patients in the test

Sensitivity

Figure 5.21 shows the sensitivity with which the detector was able to detect the seizures from the 10 patients in the test. Overall 91.49% of the test seizures were detected.

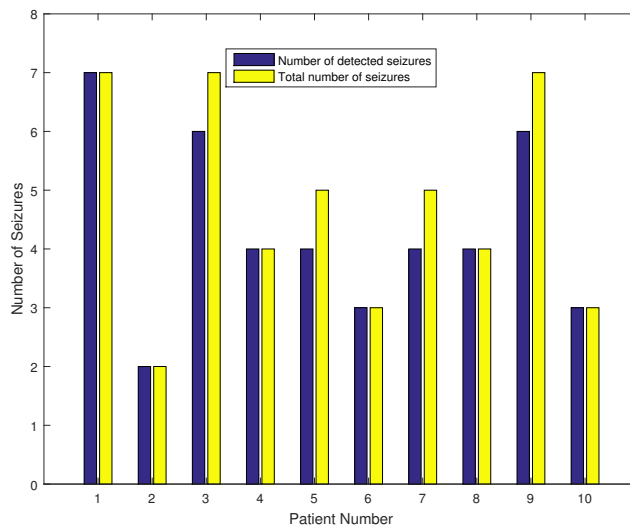


FIGURE 5.21: Detector sensitivity for the 10 patients

Chapter 6

Conclusions And Future Work

6.1 Conclusions

The objective of this thesis was to discuss the feasibility of a system for the detection of epileptic seizures. The system was based on the estimation of the number of optimum embedding dimensions used for the recreation of an attractor of a non linear dynamic system. The non linear dynamic system was created by fusing together the data from all EEG channels by the assumption that the each and every frequency component of the EEG was generated by a single dipole source. The Stockwell transform and the Global Field Power measurement was used for this purpose.

Preliminary test showed that the detection method was able to detect the occurrence of an epileptic seizure and further testing showed that the system had a detection sensitivity of 91.49% for the EEG recordings used. A mean seizure detection time of 3.59 seconds was reported. The false detection rate of the system was not considered as there was no way to ascertain if any of the false detections were actually sub clinical seizures that were not reported in the original dataset. This decision was reached after the EEG segments that generated the false detections in the preliminary tests were viewed and found to

closely resemble those of sub clinical seizures which were published in reputed medical journals.

The proposed detection method did not need much customization from patient to patient other than identifying the the preictal optimum embedding dimension range that the systems attractor occupied in phase space. Although the detection system appears to be promising, long testing on a much larger varied dataset will be required to gauge its true potential.

6.2 Future Work

1. Test the feasibility of using perpetual points in the attractor as a method of detecting where bifurcations occur. A perpetual point in an attractor is a point where the velocity and acceleration of the change in states along an attractor trajectory are instantaneously zero, in contrast to fixed points where only the velocity is instantaneously zero. Perpetual points have been recently shown to indicate bifurcations of attractors in phase space [Prasad2015]. Therefore the acceleration and velocity along an optimally embedded reconstructed attractor are calculated and any perpetual points are identified as a method of searching for bifurcations in the EEG attractor caused by seizures.
2. Long term testing is need to verify the operation of almost all newly designed systems, therefore as a first step in the future for this proposed system would be to test it on a widely varied EEG data set containing not only epileptic seizures, but also all the irregularities and artefacts that are possible to be recorded. Only then will the true flaws in this system be revealed, which then can be corrected.

3. This detection method requires extensive computing power in its current form. therefore for it to be truly practically implemented further research is needed to as to how it can be implemented as an embedded system. Parallelizing the processing on a Field Programmable Gate Array (FPGA) thus seems a logical step.

4. Easy to use wearable brain computer interface devices such as the Emotiv Epoc+ 14 channel EEG device are now available. Coupling an embedded system that implements the proposed detection method will create a portable epileptic seizure detection system that can be field tested, thus possibly leading to the development of a commercial product.